Chapter 24
Synergic Combinations of Computational Methods and Experiments for Structural Diagnoses

Giulio Maier, Gabriella Bolzon, Vladimir Buljak, Tomasz Garbowski, and Bartosz Miller

Abstract. The mechanical characterization of materials and the non-destructive assessment of possible damages in industrial plant components and in civil engineering structures and infrastructures is a problem which at present arises more and more frequently and acquires growing importance in both experimental and computational mechanics. The survey presented here concerns some representative, practically meaningful typical problems of this kind recently or currently tackled by our research team. It is intended to evidence the central role played by computer methods and by procedures of numerical mathematics, including soft computing, for the practical solutions of inverse analysis problems in real-life situations. The engineering applications dealt with herein concern steel pipelines and metal industrial components typical of the oil industry and existing large concrete dams possibly deteriorated by physico-chemical processes like alkali-silica reactions.

Giulio Maier
Department of Structural Engineering, Politecnico (Technical University) di Milano, piazza Leonardo da Vinci 32, 20133 Milano, Italy
e-mail: maier@stru.polimi.it

Gabriella Bolzon
Department of Structural Engineering, Politecnico (Technical University) di Milano, piazza Leonardo da Vinci 32, 20133 Milano, Italy
e-mail: bolzon@stru.polimi.it

Vladimir Buljak
Department of Structural Engineering, Politecnico (Technical University) di Milano, piazza Leonardo da Vinci 32, 20133 Milano, Italy
e-mail: buljak@stru.polimi.it

Tomasz Garbowski
Department of Structural Engineering, Politecnico (Technical University) di Milano, piazza Leonardo da Vinci 32, 20133 Milano, Italy
e-mail: thomas@stru.polimi.it

Bartosz Miller
Department of Structural Mechanics, Rzeszów University of Technology, ul. Poznańska 2, 35-959 Rzeszów, Poland
e-mail: bartosz.miller@prz.edu.pl

M. Kuczma, K. Wilmanski (Eds.): Computer Methods in Mechanics, ASM 1, pp. 453–476.
springerlink.com

24.1 Introduction

In most practical situations including the real-life problems considered herein, the following circumstances characterize parameter identifications: (i) a finite domain containing the sought parameters can a priori be specified in their space (some times by an "expert" in the field), at least through lower and upper bounds on each parameter; (ii) correlation generally holds among the vectors of measurable quantities belonging to the responses of the system with differences only among parameters within the above mentioned domain; such vectors are "correlated" in sense that they turn out to be "almost parallel" in their space.

The mathematical and computational methods listed below (and described in referenced publications) have been employed to solve the practical parameter identification problems here outlined in Sect. 24.2 and Sect. 24.3 and can be regarded, at present or in the near future, as central in most inverse problems in structural engineering.

(a) The correlation reasonably expected among response vectors, as above noticed by remark (ii), makes potentially fruitful in the present context the recourse to Proper Orthogonal Decomposition (POD). Such procedure of growing interest in mechanics, can be summarized as follows (for details see e.g. [10, 22, 26, 27]): starting from say M points ("nodes") in the P-dimensional domain of the sought parameters, let experiment simulations (or, very seldom, true experiments) lead to the M corresponding vectors ("snapshots" in the POD jargon), each one of N measurable response quantities. As suggested by the correlation of the snapshots gathered in the $N \times M$ matrix $\mathbf{U}$, new Cartesian reference axes are determined such that, sequentially, a norm of the snapshot projections on each of them is made maximal; thereafter a "truncation" is carried out, namely only $\overline{N}$ axes with non-negligible component norms are preserved. Such procedure computationally implies the calculation of eigenvalues and eigenvectors of the (symmetric, positive semidefinite) matrix $\mathbf{U}^T\mathbf{U} = \mathbf{D}$. After this central computing effort, the "truncation" based on a comparative assessment of the above eigenvalues leads to a $N \times \overline{N}$ matrix $\overline{\mathbf{\Phi}}$ with $\overline{N} \ll N$, which represents new "truncated" Cartesian reference. Thereafter, the snapshot "amplitudes" in the new reference are easily computed and gathered in $\overline{N} \times M$ matrix $\overline{\mathbf{A}}$.

(b) Suppose that computer simulations of the system response have been carried out by conventional modeling (say by a finite element code) on the basis of parameter vectors belonging to a suitable node grid on the domain in the P-dimensional parameter space. Then the system response based on a new parameter P-vector $\mathbf{p}$ (namely the amplitude vector $\overline{\mathbf{a}}$ which defines the relevant snapshot $\mathbf{u}$) can be computed by interpolation of the available results much more economically than by a further direct analysis through the conventional forward operator. Such interpolation can be efficiently performed by expressing the sought vector $\overline{\mathbf{a}}(\mathbf{p})$ as a linear combination of Radial Basis Functions (RBF) (see e.g. [8, 27]). In the present study the selected RBFs are axially symmetrical functions of the "distances" (Euclidean norm) between the point $\mathbf{p}$ and the grid nodes in the parameter space $\mathbf{p}_i$, $i = 1, ..., M$. The $\overline{N} \times M$ interpolation coefficients of such linear combinations are solutions to

the linear equation system arising from the obvious requirement that the amplitude vector function equals the known amplitude $\overline{N}$-vector $\overline{\mathbf{a}}(\mathbf{p})_i$ in each node of the grid.

(c) Among the several first-order procedures now available in the broad literature on Nonlinear Mathematical Programming (NMP), the Trust Region Algorithm (TRA) has been selected to the present purposes. Its main features can be briefly pointed out as follows: at each iteration a two-variable quadratic programming problem is solved over the (hyper) plane defined by the gradient and by the Newton vector of the discrepancy function to minimize; the quadratic approximation of the objective function is generated by an approximation of the Hessian computed through the Jacobian of the "errors" (errors mean here differences between measurable and computed quantities, the latter computed as functions of the sought parameters); repeated diverse initializations have fragmentarily to be performed in order to avoid end of the step sequence in a local minimum different from the global one, due to possible lack of convexity. On TRA and on other NMP algorithms of first order (and of diverse orders, in particular of zero order or "direct search" like Nelder-Mead or "complex" algorithms) details can be found e.g in [11, 16].

(d) The possible presence of local minima and the presence of a domain "a priori" predictable in the space of the unknowns, clearly make Genetic Algorithms (GA) pertinent and promising conceptual and computational tools in the present context. On the other hand, Artificial Neural Networks (ANN) turn out to be of obvious interest for the engineering applications pursued herein, in view of the significant advantages provided by structural diagnosis made repeatedly "in situ" by a portable computer endowed with an ANN "trained" and "tested" once for all originally in a computer laboratory. In the vast literature on GA and ANN and on soft computing in general, references [19, 29] are among the primary sources of information for what follows.

24.2 Local Diagnostic Analyses of Concrete Dams

24.2.1 Preliminary Remarks

The possible deterioration of existing concrete dams gives rise at present, and probably even more in the future, to real challenges in structural engineering, especially in developed countries where a multiplicity of large dams have been designed and built up several decades ago. The main causes of most damages in concrete dams are extreme loadings, such as earthquakes and floods, slow orogenetic motions of geological surroundings and, the most dangerous one, Alkali Silica Reaction (ASR). The physico-chemical process ASR, not clearly understood before the end of the Eighties, is generally dormant during one decade or more after casting, and later gradually reduces, sometimes to a large extent, concrete stiffness and strengths and generates irreversible expansions and consequent self-equilibrated stresses, see e.g. [2, 12].

Statical overall diagnostic analyses are based on measurements (by pendula and collimators or in the near future by radar) of displacements generated either by quasi-static loading due to reservoir level variations ("ad hoc" fast, see e.g. [15]; or seasonal in service, see e.g. [4]). Dynamical overall diagnoses are based on excitations by vibrodynes and measurements by accelerators. Clearly, only elastic moduli (Young modulus alone in practice), assumed as zone-wise uniform, can be assessed by overall, statical or dynamical, nondestructive testing and inverse analyses.

Inelastic properties of concrete and stresses in existing dams can be assessed by local "nondestructive" tests. These are briefly considered in what follows in order to evidence the potential improvements due to applications of recent developments in computational inverse analysis methodologies mentioned in the Introduction.

24.2.2 Tests on Dam Surfaces by Flat-Jacks

Flat-jack tests are frequently applied to performed masonry structures and concrete dams since several decades. The state of the art of this popular procedure can be outlined as follows, see e.g. [17]:
(α) two parallel circumferential slots are digged;
(β) the cuts alter the existing stress state and the consequent elongations between marked points in direction orthogonal to the slots are measured by extensometers;
(γ) a flat-jack is inserted and pressurized until the previously measured elongations are fully recovered and, hence, the jack pressure approximately equals (to within a corrective empirical factor accounting for the jack geometry and welds) the compressive stress pre-existing there;
(δ) flat-jacks are inserted in both slots and pressurized: the pressure related to consequent measured elongations leads, again through semi-empirical formulae, to an estimation of the Young modulus;
(ε) estimations of Young modulus and, usually assumed "a priori", of Poisson ratio, can be employed for an assessment of the normal stress on the basis of the elongation measurements in phase (α), as an alternative (or as a validation) of the stress estimation at phase (γ).

To comparison purposes, a brief description is presented here below of the novel flat-jack diagnostic procedure made possible by progress in both computational and experimental mechanics. This procedure is novel also in terms of extension to plasticity and fracture and of experimental equipment, with recent innovative proposals described in [13, 14].
(I) Two slots are digged, one orthogonal to the other ("T geometry") without intersection.
(II) A conventional three-dimensional FE model is generated "una tantum" over a suitable domain with constrained boundary conditions in unperturbed zone;
(III) The consequent perturbation of the stress state gives rise to elastic displacements; these are measured on the surrounding surface by Digital Image Correlation

(DIC) at the nodes of suitable designed grid, nodes which are coincident with nodes of the FE mesh.
(IV) The jacks are inserted into the slots and moderately pressurized; the consequent elastic displacements are measured by DIC.
(V) The pressure is increased in order to cause inelastic deformations, including fracture propagation, particularly between the two slots. Once again displacements are measured by DIC.
(VI) Inverse analysis based on the experimental data gathered in phase (IV) identifies elastic moduli.
(VII) The elastic moduli identified at the stage (VI) are employed for the estimation of stresses on the basis of DIC measurements in stage (III).
(VII) Finally, the inelastic and fracture behavior of concrete is characterized by means of inverse analysis by exploiting the experimental data collected through DIC during phase (V).

The above outlined innovative procedure has been validated by a number of "pseudo-experimental" exercises, namely: numerical values are assigned to the sought parameters; on this basis a computer simulation of the test generates measurable quantities; starting from these quantities inverse analysis leads to parameter estimates which are compared to the originally assumed values. A representative validation exercise is briefly described below (details will be available in journal papers).

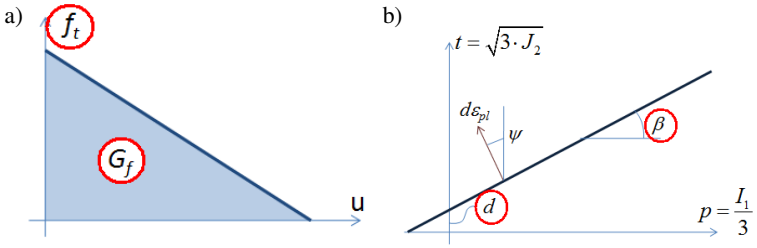

Fig. 24.1 Inelastic parameters to identify in single cohesive crack **a** and Drucker-Prager **b** model for concrete

In the elastic range, orthotropic and horizontally isotropic behavior is attributed to concrete, in view of possible consequences of the casting process (and, in some cases, of roller compaction). Specifically, in the reference frame with axes x and y on the dam surface and x and z on horizontal plane, the elastic moduli which govern the Hooke's law and the values assumed for them are: $E_x = E_z = E_H = 20\,\text{GPa}$; $E_y = E_V = 30\,\text{GPa}$; $G_{xy} = G_{yz} = G_V = 9.6\,\text{GPa}$; $\nu_{xz} = \nu_H = 0.2$; $\nu_{yx} = \nu_{VH} = 0.2$; $\nu_{xy} = \nu_{HV} = \nu_{VH}\frac{E_H}{E_V} = 0.3$. The shear modulus in the isotropy plane $G_{xz} = G_H = 8.33\,\text{MPa}$ depends on ν_H and E_H.

The parameters to identify are E_H, E_V and G_V, since the Poisson ratios ν_H and ν_{VH} are assumed a priori known in view of their marginal influence on structural responses.

In the inelastic range the simplest cohesive crack model of Fig. 24.1a is adopted for the expected mode I quasi-brittle fracture propagation. The parameters to identify are tensile strength f_t and fracture energy G_f, originally assumed equal to 3 MPa and 150 N/m, respectively, for initial forward analyses in view of pseudo-experimental validation.

The simplest plasticity model is considered for concrete in the plastic range, namely Drucker-Prager yield criterion and flow potential:

$$F = t - p\tan(\beta) - d \leq 0\,; \quad G = t - p\tan(\psi) \tag{24.1}$$

where p is the mean normal stress and t the equivalent shear stress (Fig. 24.1b). The dilatancy angle is a priori assumed $\psi = 40\,\text{deg}$. The internal friction angle β (Fig. 24.1b), originally assumed $\beta = 68\,\text{deg}$, is the third parameter to identify, together with f_t and G_f, since the cohesion d and compression strength f_c are not independent but related to the above parameters as follows:

$$f_c = \frac{d}{1 - \frac{1}{3}\tan(\beta)} = \frac{\left(1 + \frac{1}{3}\tan(\beta)\right) f_t}{1 - \frac{1}{3}\tan(\beta)} \tag{24.2}$$

It is worth noting that the simplicity here adopted in material models is consistent with the novelty of the proposed flat-jack procedure and with the uncertainties of the experimental data achievable in the engineering context of large concrete dams.

As for stresses to estimate, plane state represents an obviously reasonably hypothesis. Therefore in the previously introduced reference axes $\sigma_z = \tau_{yz} = \tau_{zx} = 0$, and, hence, sought components are $\sigma_H = \sigma_x$, $\sigma_V = \sigma_y$, $\tau = \tau_{xy}$, with the following assumption for numerical pseudo-experimental checks: $\sigma_H = -2\,\text{MPa}$, $\sigma_V = -6\,\text{MPa}$, $\tau = 1\,\text{MPa}$.

The adopted finite element model, visualized in Fig. 24.2, exhibits the following features: 60,400 tetrahedral FEs; 47,200 DOF; zero displacements on the boundary supposed to be not influenced by the test.

Digital Image Correlation (DIC) is an optical technique developed for full-field measurements of surface displacements (see e.g. [28]). It is based on comparison between two images of specimen taken in the undeformed and deformed state. Correlation between material points (actually small zones) in the undeformed and deformed images is obtained over the "Zone Of Interest" (ZOI) by an image-matching procedure based on gray levels stored in "pixels".

With respect to the extensometers employed so far in flat-jack tests and to other optical measurement methods, the special merits of DIC are: non-contact measurements; simple optic setup; no special preparation of specimens; no special illumination; smaller measurement "noise". Moreover, for the present inverse analysis method meaningful advantage is provided by the substantial increase of the experimental data number and consequent regularization (in Tikhonov sense [9]) of the discrepancy minimization problem.

Figure 24.3 visualizes the operative experimental phases of the proposed flat-jack method. Over the ZOI shown in Fig. 24.4 photographs for DIC are taken at

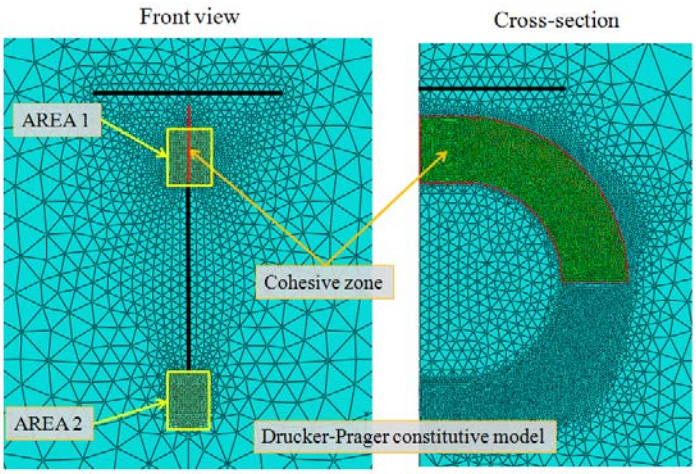

Fig. 24.2 Finite element model for simulations of the flat-jack tests. Areas 1 and 2 are concerned by DIC measurements during the inelastic phases of the test

stage (a), with only marks of slots before digging, and at stage (b) in the presence of the still empty slots; then at phase (c) after jack insertion and pressurization. The ZOI for DIC are reduced in phase (d-e) as shown in Fig. 24.4, in order to concentrate measurements near the places where plastic strains and fracture propagations are expected (i.e. over the sub-domain where inelastic material models have been adopted, as shown in Fig. 24.2).

In the present engineering context it is particularly desirable, or even necessary, that the diagnostic assessment of possible local material damage be carried out repeatedly and routinely, by using portable equipment (including computers) apt to provide all the sought estimates soon and "in situ" and in "nondestructive" fashion (in particular without specimen extraction).

Such practical requirements, besides the increase of reachable information evidenced earlier by comparison with the state-of-the-art, can be attained at present by suitable applications of the computational methods mentioned earlier in Sect. 24.1.

After a number of numerical exercises, the following computing tools have been evaluated as probably optimal for the novel flat-jack methodology proposed by our team and outlined in what precedes.

All three identification procedures are performed by exploiting Proper Orthogonal Decomposition (POD) together with Artificial Neural Networks (ANN) or with Trust Region Algorithm (TRA) through RBF interpolations. Computationally, the proposed diagnostic method proceeds according to the guidelines which follow.
(i) The three sets of numerous (N) displacements measurable by DIC are computed by FE model (see Fig. 24.2), once for all in a computing center, as "snapshots" corresponding to M nodes of the grid over the expected domain in each one of the three spaces of parameters. Specifically, in a typical numerical exercise of this study:

for elastic moduli (phase b-c, Fig. 24.3) $N = 2086$, $M = 1089$; for stresses (phase a-c) $N = 2086$, $M = 3375$; for inelastic parameters (phase d-e) $N = 238$, $M = 1620$.

Clearly, the elastic moduli, identified first, have to be inserted as data for the two subsequent identifications and, hence, they represent an increase of the number of dimensions in the space where to generate the grids of nodes. Therefore isotropy and hence only Young modulus E has been considered here in preliminary validations of procedures apt to estimate by inverse analysis inelastic parameters. The description which follows is focused on the identification of three elastic moduli, but only on it for brevity.

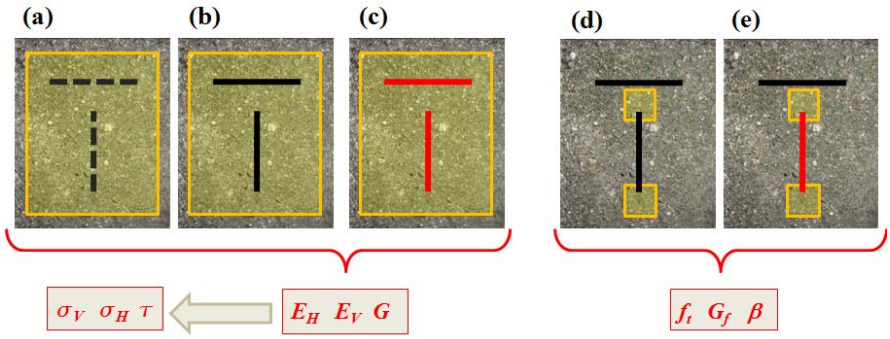

Fig. 24.3 Phase sequence in the new flat-jack testing procedure on concrete dams

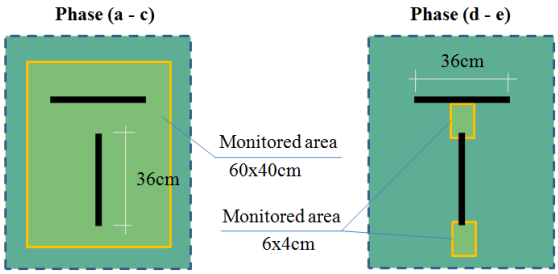

Fig. 24.4 Areas monitored by digital correlation instruments in the parameter identification stages specified in Fig. 24.3

(ii) The "compression" (in other terms approximation) of the information contents of the three large snapshot $N \times M$ matrices $\mathbf{U}$ generated once for all at phase (i), is accomplished, again once for all, by POD. The relevant "truncation" was made at an eigenvalue with order of magnitude ten thousand times less then the maximum eigenvalue.

(iii) Any new "snapshot" of truly experimental data provided in the future by DIC will be compressed to its "amplitudes" in the truncated reference system generated

by POD in phase (ii). This prospect makes computationally useful to generate a multilayer feed-forward Artificial Neural Network (ANN) once for all, in order to perform fast and "in situ" the transition from the compressed experimental data to the sought parameters; these are, at this stage, the three elastic moduli. In the present context the optimized architecture of ANN to be calibrated ("trained", "tested" and "validated") through POD generated "patterns" turned out to consist of 3-20-3 neurons in input, hidden and output layer, respectively. Other features which characterize the ANN in point are as follows: tan-sigmoid and linear transform function in hidden and output layer, respectively; "training" by a usual back-propagation procedure, Levenberg-Marquardt algorithm; the pattern set is divided into training, testing and validation subsets in the following proportions 0.6-0.2-0.2.
(iv) As an alternative to ANN, the POD procedure mentioned at (ii) has been associated also to Trust Region Algorithm (TRA), so that in its iterations requiring derivatives, direct analysis is replaced by interpolation through Radial Basis Functions (RBF). The here selected formulation of these functions reads (**p** being the vector of sought parameters):

$$g_j(\mathbf{p}) = ||\mathbf{p} - \mathbf{p}_j||^3 \tag{24.3}$$

The estimations achievable by the above methods, briefly indicated as POD-ANN and POD-RBF-TRA, have been comparatively checked from various standpoints.

For example, the influence of random noise in DIC data on consequent errors in the estimations turns out to be comparable, as visualized in Fig. 24.5: a random perturbation of DIC pseudo-experimental data with uniform probability density over the interval 10 μm leads to the perturbations of elastic parameter estimations shown in Fig. 24.5a with the former method (iii); in Fig. 24.5b with the latter procedure (iv). This comparative numerical exercise on the two different computational procedures (POD-ANN and POD-RBF-TRA) have almost equal average estimation errors (2.245% and 2.352%, respectively).

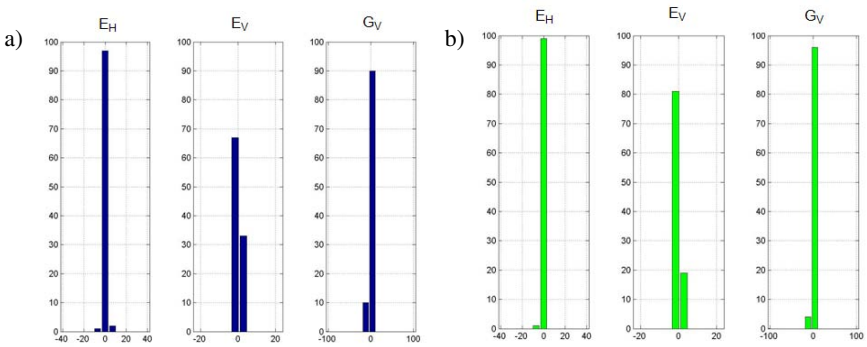

Fig. 24.5 Scattering (in percentage) of the elastic parameter estimates by POD-ANN **a** and POD-RBF-TRA **b** diagnostic procedure on the basis of some randomly perturbed pseudo-experimental data from DIC

It is reasonably expected that the displacement measurements by DIC, even if affected by same experimental errors (here $\pm 10\,\mu$m), lead to more stable and more robust estimations then those provided by extensometers. In fact, the number of the latter was reasonably assumed as limited to 16 (even less in the present practice). The above conjecture turns out to be quantified and confirmed by numerical results in Fig. 24.6a compared to the preceding Fig. 24.5a.

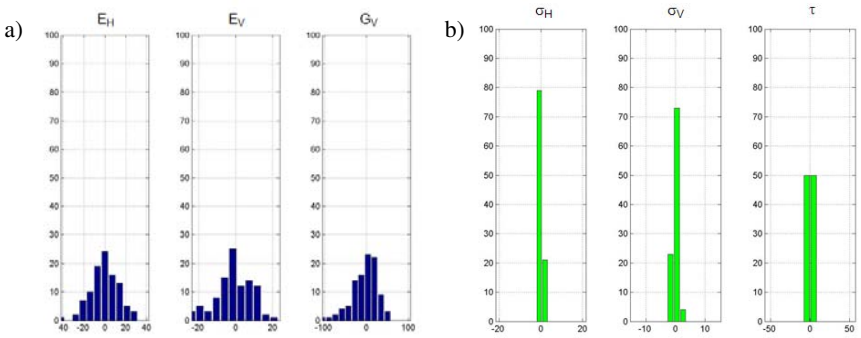

Fig. 24.6 In **a** results analogous to those in Fig. 24.5b but on basis of similarly perturbed data provided by extensometers instead of by DIC. In **b** scattering of stresses resulting from the same DIC data and POD-RBF-TRA procedure like in Fig. 24.5b, and from the averages of the elastic moduli estimates considered there

Figure 24.6b shows errors of an identification by POD-RBF-TRA based again on DIC measurements, but concerns the estimates of the three stress components after the assessment of the concrete elastic stiffness.

Finally, several numerical tests concerning the above POD-RBF-TRA procedure demonstrated that promising are estimations of the inelastic parameters specified in Fig. 24.1 when DIC provides data from stages (d-e), Fig. 24.3. Figure 24.7 illustrates convergence on the reference values when only the cohesive crack model of Fig. 24.1a is considered in the simulation beyond the elastic range, account taken of the stiffness and stresses estimate in the preceding stages (primarily here $E_H = 20\,$MPa, $\sigma_H = -3\,$MPa), Figure 24.8 shows the same convergence behavior when both cohesive and Drucker-Prager models are involved in the FE simulation of the novel flat-jack test.

24.2.3 Dilatometric Tests in Depth

Deterioration of concrete by a diffusive physico-chemical process like ASR clearly may concern the whole volume of a large dam. Damage assessment in interior castings still represents a challenge, which is tackled so far primarily by extraction of specimens to be tested in labs, according to techniques traditionally used in rock

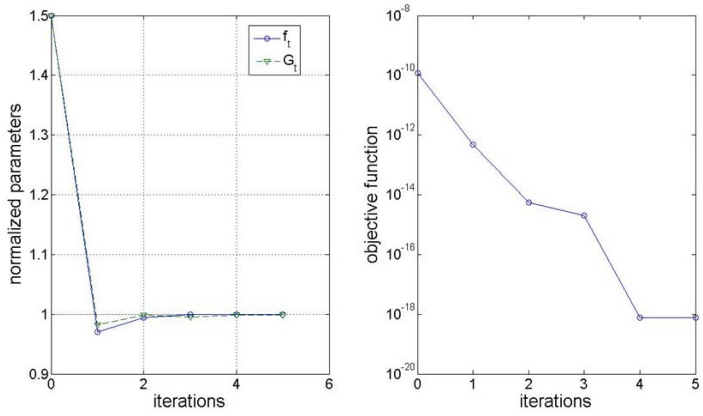

Fig. 24.7 Convergence of the Trust Region Algorithm for the estimation of concrete tensile strength f_t and fracture energy G_f (normalized by the reference values or "targets") based on DIC measurements, according to Fig. 24.4 phases (d-e)

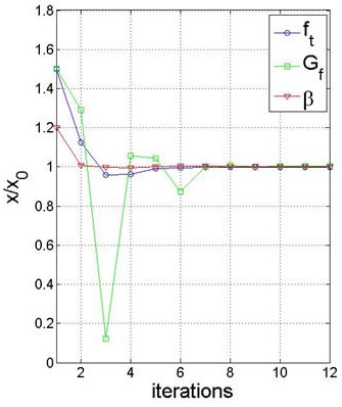

Fig. 24.8 Same as in Fig. 24.7 but by test simulation including both crack (Fig. 24.1a) and Drucker-Prager (Fig. 24.1b) models

mechanics (see e.g. [3]). Inverse analysis and relevant computational methods pointed out in what precedes inspired the procedure outlined below.

The proposed instrumentation (not yet available on the market) is schematically depicted in Fig. 24.9. It is inserted in depth after hole drilling. The experiment and relevant parameter identification are articulated in the following stages: (i) further drilling process by, say, one meter (Fig. 24.9); (ii) the consequent changes in the stress state, supposed originally uniform with prevailing transversal, horizontal σ_H and vertical σ_V, normal stresses, give rise to deformation with radial displacements which are measured by 12 gauges (called "dilatometers") included in the experimental equipment (Fig. 24.9); (iii) two pairs of radial "wedges" (or "arches"), in horizontal and vertical directions, are activated by small internal jacks and operate on the hole surface (Fig. 24.9) with a relationship force-versus-advancement like

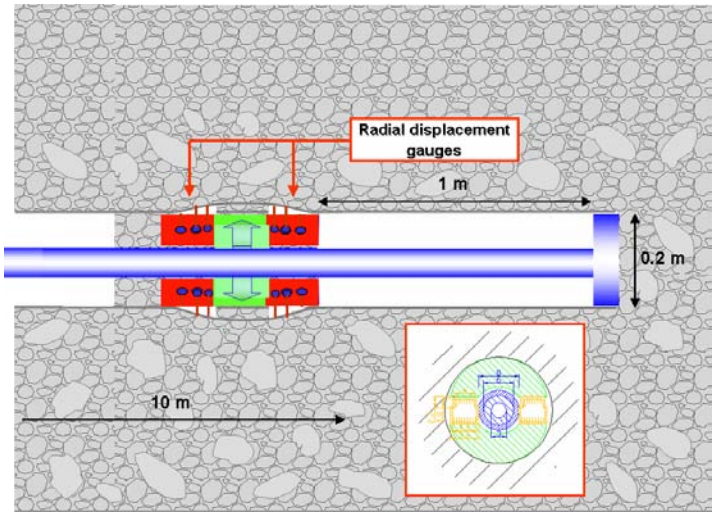

Fig. 24.9 Schematic representation of the proposed equipment for dilatometric tests in concrete dams.

the one shown in Fig. 24.10, generated by a FE simulation; (iv) the data gathered and digitalized in phase (iii) feed a POD-ANN procedure similar to the one earlier described with reference to flat-jack tests and implemented in order to estimate "in situ" the elastic moduli; (v) now the displacements measured in stage (ii) are employed for the identification of dominant stresses σ_H and σ_V by a procedure similar to the one applied at the preceding stage (iv), but using the elastic estimates produced at (iv); (vi) finally, experimental data extracted from the inelastic parts of force-versus-advancement measured relations like in Fig. 24.10 are exploited for another inverse analysis leading to parameters governing a plastic constitutive model. This model in preliminary validation exercises has been chosen same as for the flat-jack superficial diagnosis, namely Drucker-Prager model; however, the elliptic "cup" implemented in ABAQUS and in other commercial codes is added here, in view of possible dominance of compressive stresses deep in a dam. Therefore, the parameters to estimate are here 5, namely E, β and d like earlier (Fig. 24.1) and also cap position p_d and ellipse eccentricity R in the implemented Drucker-Prager model.

Identification procedures are here not described for brevity, since they are conceptually similar to those combined with flat-jack tests and specified in the preceding subsection.

Sensitivity analysis is here particularly useful in order to mitigate possible doubts on the identifiability of the present procedure. Figure 24.11 visualizes by columns the changes of the vertical wedge displacements from their maximum values (about 10 mm) when the 5 material parameters are separately varied by 5% from their reference values.

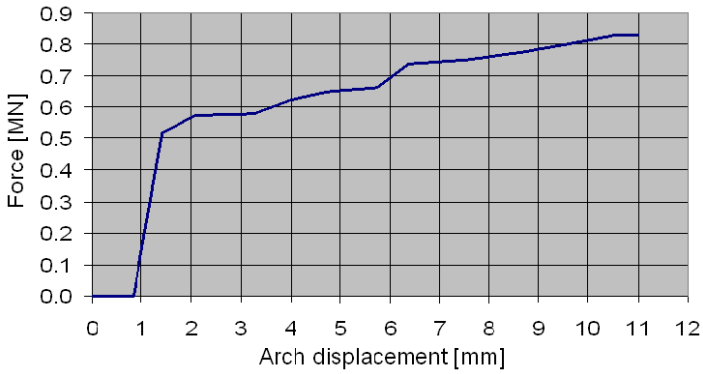

Fig. 24.10 Force versus arch advancement generated by a computer simulation of the wedging phase in the proposed dilatometric testing procedure

As a conclusion of this Section, it can be stated that current progress in computational methods applicable to inverse analysis techniques, even if they are developed by a simple deterministic approach, are likely to become substantially beneficial to the engineering practice for extensive diagnoses of large concrete dams.

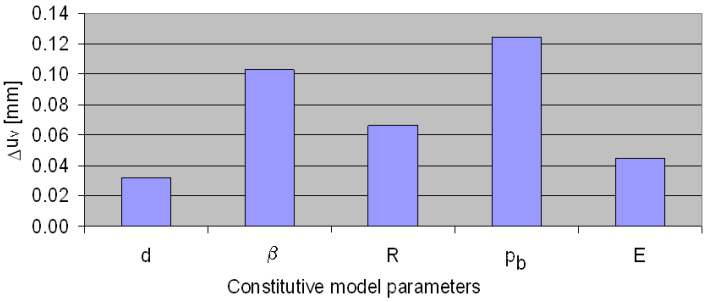

Fig. 24.11 A comparative assessment of sensitivity of dilatometric measurements (Fig. 24.9) with respect to the parameters which govern Drucker-Prager model with "cap" attributed to dam concrete

24.3 Diagnostic Analysis of Metallic Industrial Components

24.3.1 Assessments of Material Parameters by Indentation

Networks of pipelines for oil or gas transportation, steel components of power plants and of offshore structures are typical examples of meaningful engineering systems

which require inspection, monitoring and assessment of present mechanical properties in view of structural analyses apt to compute safety margins. In fact, material parameters to be input into computer modeling may be somewhere unknown or deteriorated by aging processes like corrosion. Traditional indentation tests originally devised for the assessment of hardness (which has a peculiar metallurgical rather than mechanical meaning), since years have been developed into a popular nondestructive technique for the calibration of material constitutive models either by semiempirical formulae (see e.g. [25]), or, in recent times, by test simulations and inverse analyses (see e.g. [6, 7, 18]).

It was proposed in [7] that experimental data apt to feed inverse analysis be provided not only by an instrumented indenter in terms of force versus penetration curves, but also by a laser profilometer in terms of geometric features of the residual imprint. Such enlargement of experimental information availability gives rise to the following broader spectrum of alternatives, among which an optimal option may be selected in each real-life situation of engineering practice: (i) the loading-unloading indentation plots are generated in digital form by an instrumented indenter and exploited as the only experimental data for inverse analyses which are carried out in situ by a portable computer; (ii) same as in (i) but instead of indentation plots, the imprint geometry only is measured and digitalized by a profilometer and then exploited for in situ parameter identification; (iii) imprint measurements only as in (ii), except that a mould of the imprint geometry is cast and taken to a laboratory endowed with profilometer and computer; (iv) the inverse analysis rests on experimental data from both the indentation plots and the imprint profile and it is performed either in situ or in the laboratory.

Clearly, all the above alternative procedures are "nondestructive", in the sense that no specimen is extracted and the caused damage is confined at the microscale; moreover, in view of their repetitiveness, they substantially benefit, in terms of time and resource savings, if the inverse problems are solved fast on small computers, possibly in situ. Therefore the computational procedures, apt to exploit "snapshot" correlations, as pointed out in Sect. 24.1, become practically desirable and useful in the present technological context. Such statement has been corroborated by many pseudo-experimental numerical exercises, on material parameter identification based on indentation tests including the illustrative ones which follow.

The constitutive model adopted here for the material is classical: isotropic, elastic-plastic, associative, with exponential hardening and Huber-Mises yield function. Its description for uniaxial stress state can be given as follows, according to the handbook format of the commercial FE code ABAQUS employed herein:

$$\sigma = E\varepsilon, \ \text{with} \ \varepsilon \leq \frac{\sigma_0}{E}, \ \sigma = \sigma_0^{1-n} E^n \varepsilon^n, \ \text{with} \ \varepsilon > \frac{\sigma_0}{E} \tag{24.4}$$

The reference values here attributed to the three parameters for pseudo-experimental numerical validations are typical of some steels: $\sigma_0 = 405\,\text{MPa}$; $E = 198\,\text{GPa}$; $n = 0.111$.

A conical indentation conforming with Rockwell test geometry is simulated by the axisymmetrical FE model shown in Fig. 24.12 and characterized by the

following features: 3320 degrees of freedom; zero displacements on the low plane and cylindrical boundaries; isotropic elastic indenter with $E = 1170\,\text{GPa}$, $\nu = 0.1$ (typical of diamond); Coulomb friction with coefficient equal to 0.15; finite strain nonlinearities according to ABAQUS code implementation (not discussed here).

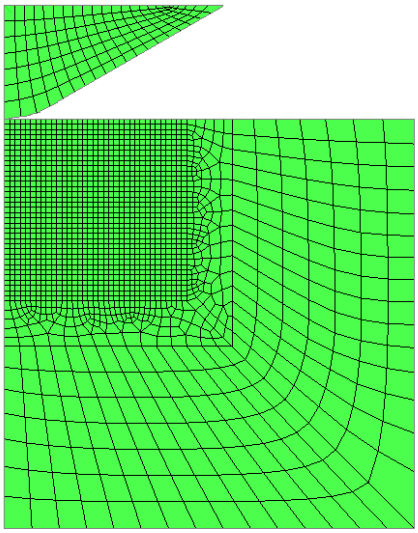

Fig. 24.12 Axi-symmetric finite element model employed for simulations of conical indentations on isotropic materials

The simulation of an indentation test by means of the above specified model leads to loading-unloading relations and imprint profile visualized in Fig. 24.13a and Fig. 24.13b respectively. The computing time was 147 seconds on the computer with the processor Intel CoreDuo 2.2 GHz with 2 GB of RAM.

The following data have been extracted from the results of the above computation: from the indentation plots 100 points of corresponding applied load and penetration depth values, assuming imposed forces at equal intervals; from the imprint profile 82 points with their two-dimensional coordinates.

The discrepancy function defined as Euclidean norm of the "errors" has been minimized first by the TRA (as mentioned in Sect. 24.1) by using at each iteration the forward operator based on the above specified FE model. Satisfactory convergence occurred, as shown e.g. in Fig. 24.14, with different initializations, which were adopted in view of possible local minima.

To investigate the influence of the noise on the inverse analysis, some moderate experimental "noise" was considered, namely randomly distributed error within the range $\pm 2\,\text{N}$ in the indentation curve, and $\pm 1\,\mu\text{m}$ in the imprint profile. Five different pairs of curves and imprints have been generated. For each case, the inverse problem was solved using the TRA with 4 different initializations. The results are presented in the Table 24.1.

In Fig. 24.15 these results are compared to the "target" (namely to a plot defined by the reference values of the sought parameters) by means of uniaxial stress-strain

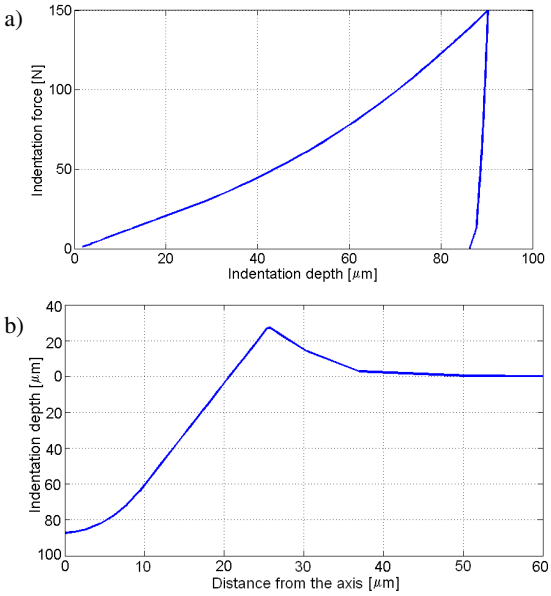

Fig. 24.13 Force on the indenter versus its penetration **a** and profile of the residual imprint **b** computed by finite element model in Fig. 24.12

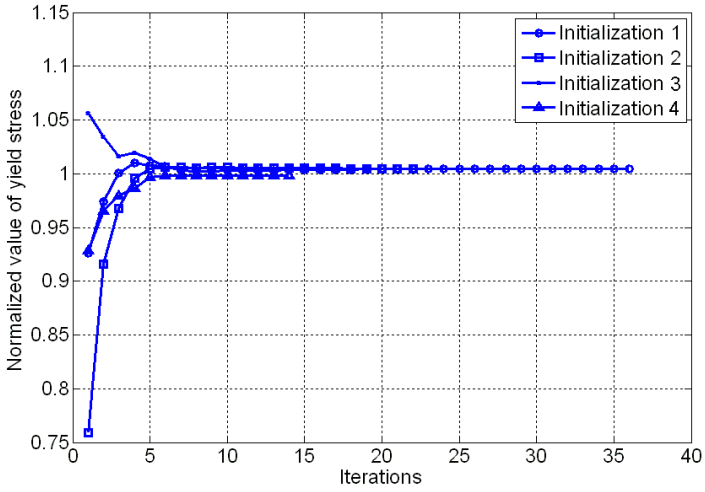

Fig. 24.14 Convergence of TRA with 4 different initializations in the inverse analysis problem based on the data visualized in Fig. 24.13

diagrams. It is worth noticing that all these curves practically coincide from an engineering perspective.

Table 24.1 Estimates and relevant standard deviations achieved through TRA from 5 diverse conical indentations on the same material modeled according to Eq. (24.4), on the basis of pseudo-experimental data randomly perturbed as specify in the text

Different cases	Young modulus	Hardening exponent	Yield stress
1	197.428 ± 8 GPa	0.10809 ± 0.0028	412.08 ± 10 MPa
2	201.170 ± 9 GPa	0.11294 ± 0.0036	401.4 ± 9 MPa
3	198.608 ± 11 GPa	0.10928 ± 0.0033	408.65 ± 7 MPa
4	190.748 ± 8 GPa	0.1114 ± 0.0033	407.01 ± 6 MPa
5	198.58 ± 5 GPa	0.1125 ± 0.0022	401.57 ± 4 MPa

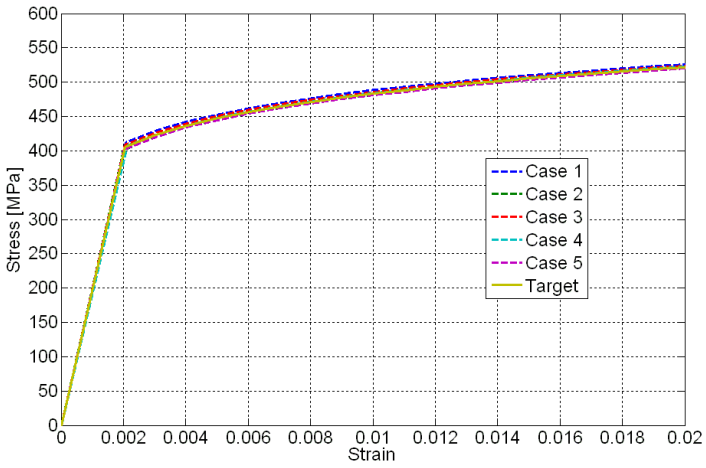

Fig. 24.15 Uniaxial stress-strain curves constructed with the estimates from the 5 initializations leading to results of Table 24.1

Also the influence of systematic modeling errors is worth being investigated beside that of random errors. To this purpose, the indentation curve and the imprint to be used as inputs in the inverse analysis are shifted upwards by increasing their ordinate values by quantities randomly generated within the range 1% and 5%. Results concerning the yield limit σ_0 in Eq. (24.4) are visualized in Fig. 24.16; in abscissa the input data sets are given, namely different material parameter combinations, while ordinate is reading the error in estimates.

The above exercises of inverse analysis by the TRA show that indentation tests do provide data suitable to estimate material parameters in isotropic elastoplasticity with hardening, according to a diagnostic procedure of kind (iv) in the test classification presented earlier. Similar numerical investigations have demonstrated that sufficient data to the same purpose can be extracted from imprint profile alone or only from loading-unloading plots. However, in all these procedures heavy computing efforts are required by repeated FE simulations within the iteration sequence of

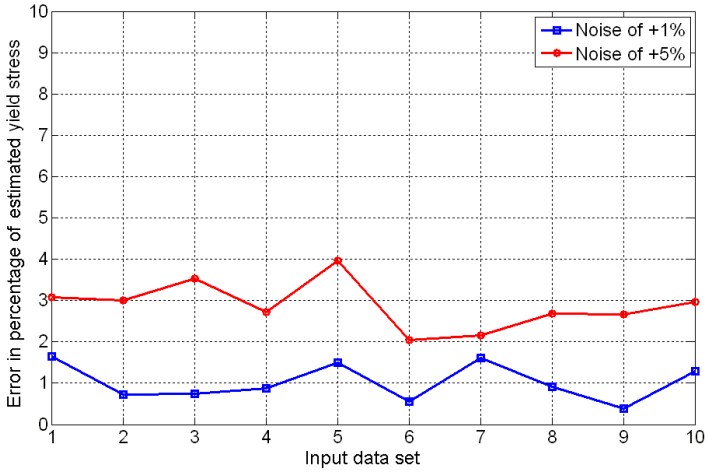

Fig. 24.16 Influence of systematic modeling error for 10 different material parameter sets

an efficient optimization algorithm like TRA or with soft-computing technique like GA (which have been tested in parallel investigations).

Therefore, as motivated in Sect. 24.1, the potential advantages in the present context of the recourse to POD and RBF have been investigated extensively by numerical exercises like those summarized here below.

First, in the three-dimensional space of the sought parameters the following grid has been generated: σ_0 from 330 MPa to 460 MPa with the step of 10 MPa; E from 170 GPa to 218 GPa with the step of 6 GPa; n from 0 to 0.2 with the step of 0.005. For each one of those "nodes" FE direct analysis has generated a vector ("snapshot") of measurable quantities in the structure response to indentation. After performing POD and computation of the "amplitudes" in the new reference system, such large information has been "compressed" by "truncation", namely dropping eigenvalues smaller than 10^{-6} times the largest one. Interpolation by RBF leads to the snapshot (through its "amplitudes") of a new parameter set: the computing time for this generation of the new response turns out to be smaller by 5 orders of magnitude, than that required to the same purpose by the conventional FE analysis.

After such very encouraging numerical tests of the above kind, POD-RBF sequence was combined first with TR algorithm. Practically the same results mentioned earlier on parameter estimations have been achieved with computing times orders-of-magnitude shorter, by means of "ad hoc" software employable in a portable computer as highly advantageous in the engineering practice referred to. The whole identification process turns out to end within couple of seconds, while it would require approximately 12 hours on the same computer if TRA is combined with FEM at each of its iterations.

Alternatively but with the same advantages pointed out above on TRA, POD has been combined with an ANN and have been investigated by similar pseudo-experimental numerical exercises of parameter estimation. The main features of here

adopted ANN is: number of neurons 12-23-3 in the input-hidden and output layers; tan-sigmoid transfer function in the hidden layer, linear in the output layer. The total number of generated patterns is the same as in previous case, 20% of them used for validation and 20% for testing; the number of data at the input of the network is 12, which represent amplitudes of the indentation curve and residual imprint in the new POD basis; output consist of the 3 sought parameters. When "clear" numerical data are used, the results of ANN exhibits exactly the same level of accuracy as those obtained by POD-RBF-TR. When noise introduced, the results turn out to be slightly worse, but from engineering point of view quite acceptable.

24.3.2 Assessment of Residual Stresses by Indentations

Residual stresses may significantly influence damaging processes, such as fatigue, and, hence durability of structures and plants. Beneficial compressive self-stress states are frequently generated near the surface of metallic industrial products, e.g. by thermal and/or chemical and/or mechanical treatments (see e.g. [20, 24]).

Various experimental techniques are now available for the quantitative assessment of residual stresses (see e.g. [5, 6, 24, 30]). When these stresses are expected to vary with depth and such variation has to be quantified, repeated indentations and inverse analysis can be advantageous in engineering practice. The proposed procedure is here pointed out by following pseudo-experimental exercise concerning a metallic shaft to which Huber-Mises model is attributed with Young modulus 200 GPa, Poisson ratio 0.3 and yield stress 1060 MPa.

Fig. 24.17a visualizes the adopted parameterization of the dependence on depth of the radial stress σ, of the assumed axi-symmeteric distribution. Analytically, such parametrization reads:

$$\sigma(x) = \sigma_{max} \sin\left(f x^m + p\right), \;\; 0 < x < d_0 \tag{24.5}$$

where

$$p = \arcsin \frac{\sigma_{sur}}{\sigma_{\max}}, \;\; f = \frac{\pi - p}{d_0^m} \tag{24.6}$$

$$m = \left(\log \frac{d_{max}}{d_0}\right)^{-1} \log \frac{\pi/2 - p}{\pi - p} \tag{24.7}$$

The parameters to identify are σ_{max}, σ_{sur}, d_0 and d_{max} listed in Table 24.2. Three indentation tests are supposed to be carried out with depths 20, 50 and 150 µm, and the force versus penetration relationships are computed by an axially symmetric FE model with 14,566 DOF (Fig. 24.17b) in order to generate the pseudo-experimental data.

The inverse problem is first solved by Trust Region optimization algorithm using as a direct operator FE simulation. Several inverse analyses have been performed with different initializations. Table 24.2 lists the obtained mean values together with

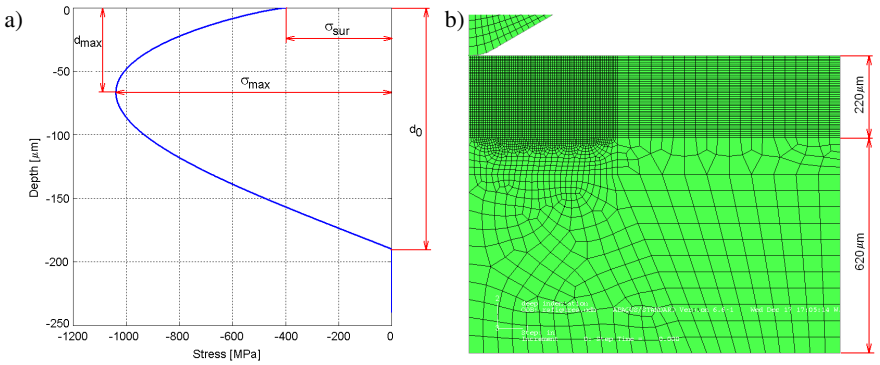

Fig. 24.17 Dependence of residual axi-symmetric stress on depth and its parameterization in **a**. In **b** the finite element model here adopted for the parameter identification

the standard deviations of the four parameters which govern the parameterized depth dependence of residual stresses.

Table 24.2 Stochastic assessment of the influence of initialization on the estimates of the residual stress parameters in Fig. 24.17a

	Mean value	Reference value (Error)
Maximal stress σ_{max}	948 ± 30 MPa	1040 MPa $(8.8 \pm 2.8\%)$
Stress at the surface σ_{sur}	429 ± 32 MPa	400 MPa $(7.25 \pm 8\%)$
Depth at which stress changes the sign d_0	209 ± 5 µm	190 µm $(10 \pm 2.6\%)$
Depth at which maximum occurs d_{max}	68 ± 6 µm	67 µm $(1.5 \pm 8.9\%)$

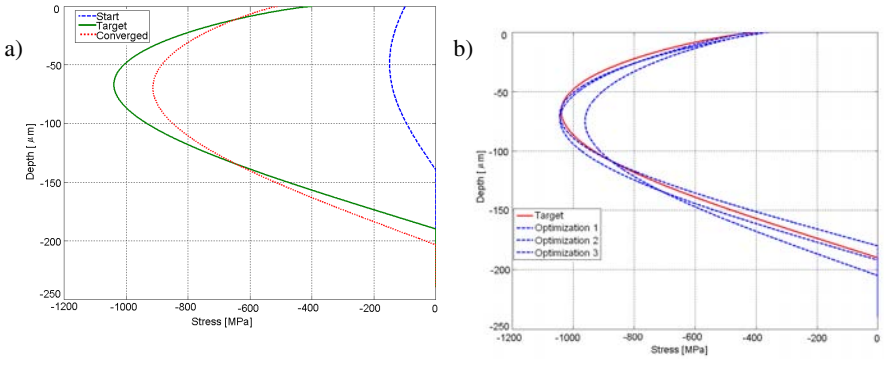

Fig. 24.18 Estimation accuracy visualized comparatively for inverse analyses: by means of TRA **a** and by GA **b**, on the basis of the same set of data and from same models of Fig. 24.17

The problem under consideration turns out to have a number of local minima, and this circumstance can explain the scattering of the numerical results presented in Table 24.2. The same identification problem has been tackled by employing a Genetic Algorithm (GA) as the tool for minimization of the discrepancy function.

In view of the large number of direct analyses generally required by GA here again a POD-RBF procedure is used. The computations of snapshots are performed through the same FE model depicted in Fig. 24.17b, by a total of 768 analyses with: σ_{max} from 500 MPa to 1060 MPa, step 80 MPa; $\frac{\sigma_{sur}}{\sigma_{max}}$ from 0.2 to 0.8, step 0.2; d from 100 µm to 220 µm, step 40 µm; and m from 0.4 to 1.4, step 0.2. For each indentation test the two snapshot matrices are generated, $\mathbf{U}_1$ $[162 \times 768]$ collecting data from the residual imprint, and $\mathbf{U}_2$ $[200 \times 768]$ for the indentation curve. The POD bases are constructed for both snapshot matrices, by truncating the one for the residual imprint after 5^{th} term, and the one for the indentation curve after 6^{th} term. The inverse multiquadric RBF here selected reads:

$$g_i(\mathbf{p}) = \frac{1}{\sqrt{||\mathbf{p} - \mathbf{p}_i||^2 + r^2}} \tag{24.8}$$

where $r = 0.5$ represents a smoothing coefficient. Results from three different GA optimizations are visualized in Fig. 24.18b. A comparison with those previously achieved, Fig. 24.18a, would suggest that GA is preferable with respect to TRA to the present purpose, in view of its insensitivity as for local minima. But both procedures for discrepancy function minimization turn out to require POD in practical applications.

24.4 Closing Remarks

The two kinds of engineering situations dealt with in what precedes are representative of a growing area of inverse analysis applications where mechanical characterization of structural materials is important and may become crucial. Other issues of current research by our team concern parameter of free-foils (especially geo-membranes and paper) [1] and ceramics and coatings [23]. The advantages provided by recent developments in computational methodology (like POD-RBF and soft computing) combined with non-traditional experimental equipments and techniques, include enlargement of the identifiable parameters set, and saving in resources and time, like e.g. when the whole procedure becomes performable "in situ" rather than in laboratory. Such advantages turned out here to be reachable by the flat-jack and dilatometric techniques for local diagnosis on concrete dams, superficially and in depth (Sect. 24.2) and by the indentation techniques applicable to industrial plants in order to identify material constitutive parameters and residual stresses (Sect. 24.3).

Deterministic approaches only have been adopted here in both sections. However, similar computational advantages due to techniques like POD and RBF exploiting

response correlation (Sect. 24.1) are reasonably expected also with stochastic approaches (i.e. assessment not only of estimates, but also of their covariance matrix which quantifies their uncertainties due to the random noise on experimental data). Severe computing efforts are likely to be mitigated also, and even more, in practical applications of stochastic techniques, like Monte Carlo, Bayesian and Kalman parameter identifications.

Sensitivity analysis (see e.g. [21]) is another meaningful subject for parameter estimation which was considered herein only in passing. The design of the experiment and in particular, the selection of the measurable quantities to be actually measured in the tests, rests primarily on numerical derivatives of them with respect to the sought parameters: hence, once again, interpolations instead of "ex novo" direct analyses are economically attractive, even if sensitivities are to be assessed once for all, rather then routinely.

The two inverse analysis problems and the relevant methodological novelties herein considered in Sect. 24.2 and Sect. 24.3 are susceptible to the following future developments, which are subject of research in progress. The flat-jack method described in Sect. 24.2 might be advantageously applied to periodic masonry if combined with homogenization procedure. The indentation techniques dealt with in Sect. 24.3 will be investigated in dynamics as well; in fact a dynamical non-instrumented indenter (like for traditional hardness tests by impact) would be by far more economical than the quasi-static ones to use for nondestructive tests "in situ", since no contrast would be required in order to generate an imprint to analyze. Finally, another promising prospect might be represented by dynamical indentation employed to mechanically characterize bricks and mortar separately in periodic masonry, in order to calibrate constitutive models for overall structural analysis by a multi-scale approach.

Acknowledgements. Research by our team in structural engineering of large dams (Sect. 24.2) and on diagnostic analysis of pipelines (Sect. 24.3) are supported by the Italian Ministry of University and by the companies Venezia Tocnologie and ENI, respectively. The authors thank the students (in particularly Ms Ada Zirpoli) who contributed by thesis works several computational exercises useful for the validation of the methodology presented herein.

References

[1] Ageno, M., Bolzon, G., Maier, G.: Mechanical characterisation of free-standing elastoplastic foils by means of membranometric measurements and inverse analysis. Structural and Multidisciplinary Optimization 38, 229–243 (2009)

[2] Ahmed, T., Burley, E., Rigden, S., Abu-Tair, A.: The effect of alkali reactivity on the mechanical properties of concrete. Construction and Buliding Materials 17, 123–144 (2003)

[3] Amadei, B., Stephansson, O.: Rock stress and its measurements. Champion and Hall, London (1997)

[4] Ardito, R., Maier, G., Massalongo, G.: Diagnostic analysis of concrete dams based on seasonal hydrostatic loading. Engineering Structures 30, 3176–3185 (2008)
[5] Bocciarelli, M., Maier, G.: Indentation and imprint mapping method for identification of residual stresses. Computational Materials Science 39, 381–392 (2007)
[6] Bolzon, G., Bocciarelli, M., Chiarullo, E.J.: Mechanical characterisaion of materials by microindentation and AFM scanning. In: Bhushan, B., Fuchs, H. (eds.) Applied Scanning Probe Methods XII - Characterization. Springer, Berlin (2008)
[7] Bolzon, G., Maier, G., Panico, M.: Material model calibration by indentation, imprint mapping and inverse analysis. International Journal of Solids and Structures 41, 2957–2975 (2004)
[8] Buhmann, M.D.: Radial Basis Functions. Cambridge University Press, Cambridge (2003)
[9] Bui, H.D.: Inverse problems in the mechanics of materials: an introduction. CRC Press, London (1994)
[10] Chatterjee, A.: An introduction to the proper orthogonal decomposition. Current Science 78(7), 808–817 (2000)
[11] Coleman, T.F., Li, Y.: An interior trust region approach for nonlinear minimization subject to bounds. SIAM Journal of Optimization 6(2), 418–445 (1996)
[12] Comi, C., Fedele, R., Perego, U.: A chemo-thermo-damage model for the analysis of concrete dams affected by alkali-silica reaction. Mechanics of Materials 41(3), 210–230 (2009)
[13] Fedele, R., Maier, G.: Flat-jack test and inverse analysis for the identification of stress states and elastic properties in concrete dams. Meccanica 42, 387–402 (2007)
[14] Fedele, R., Maier, G., Miller, B.: Identification of elastic stiffness and local stresses in concrete dams by in situ tests and neural networks. Structure and Infrastructure Engineering 1(3), 165–180 (2005)
[15] Fedele, R., Maier, G., Miller, B.: Health assessment of concrete dams by overall inverse analyses and neural networks. Int. J. of Fracture 137, 151–172 (2006)
[16] Giannessi, F.: Constrained optimization and image space. Springer, New York (2005)
[17] Gregorczyk, R., Lourenco, P.B.: A review on flat-jack testing. Engenharia Civil 9, 39–50 (2000)
[18] Gu, Y., Nakamura, T., Prchlik, L., Sampath, S., Wallace, J.: Micro-indentation and inverse analysis to characterize elastic-plastic graded materials. Materials Science and Engineering 345, 223–233 (2003)
[19] Haykin, S.: Neural networks: A Comprehensive Foundation, 2nd edn. Prentice Hall, Englewood Cliffs (1998)
[20] James, M.N., Hughes, D.J., Chen, Z., Lombard, H., Hattingh, D.G., Asquith, D., Yates, J.R., Webster, P.J.: Residual stresses and fatigue performance. Engineering Failure Analysis 14, 384–395 (2007)
[21] Kleiber, M., Antunez, H., Hien, T.D., Kowalczyk, P.: Parameter sensitivity in non-linear mechanics. John Wiley, Chichester (1997)
[22] Ly, H.V., Tran, H.T.: Modeling and control of physical processes using proper orthogonal decomposition. Mathematical and Computer Modeling 33, 223–236 (2001)
[23] Maier, G., Bocciarelli, M., Bolzon, G., Fedele, R.: Inverse analyses in fracture mechanics. Plenary Lecture, 11th International Conference on Fracture. Int. J. of Fracture 138, 47–73 (2006)
[24] McClung, R.C.: A literature survey on the stability and significance of residual stresses during fatigue. Fatigue & Fracture of Engineering Materials and Structures 30(3), 137–205 (2007)

[25] Oliver, W.C., Pharr, G.M.: An improved techniques for determining hardness elastic modulus using load and displacement sensing indentation experiments. Journal of Materials Research 7, 176–181 (1992)
[26] Ostrowski, Z., Białecki, R.A., Kassab, A.J.: Estimation of constant thermal conductivity by use of Proper Orthogonal Decomposition. Computational Mechanics 37, 52–59 (2005)
[27] Ostrowski, Z., Białecki, R.A., Kassab, A.J.: Solving inverse heat conduction problems using trained POD-RBF network. Inverse Problems in Science and Engineering 16(1), 705–714 (2008)
[28] Réthoté, J., Hild, F., Roux, S.: Extended digital image correlation with crack shape optimization. International Journal for Numerical Methods in Engineering 73, 248–272 (2008)
[29] Waszczyszyn, Z.: Neural networks in the analysis and design of structure. Springer, Wien, New York (1999)
[30] Zhao, F., Huang, Y., Hwan, K.C.: Determination of uniaxial residual stress and mechanical properties by instrumented indentation. Acta Materialia 54(10), 2823–2832 (2006)